Design, Analysis and Performance of a Rotary Wing MAV

Felipe Bohorquez, Paul Samuel, Jayant Sirohi, Darryll Pines,* Lael Rudd
Smart Structures Laboratory, Alfred Gessow Rotorcraft Center
Department of Aerospace Engineering, University of Maryland
College Park, MD 20742

Ron Perel
Johns Hopkins University/Applied Physics Laboratory
Laurel, MD 20725

Abstract

An initial design concept for a micro-coaxial rotorcraft using custom manufacturing techniques and commercial off-the-shelf components is discussed in this paper. Issues associated with the feasibility of achieving hover and fully functional flight control at small scale for a coaxial rotor configuration are addressed. Results from this initial feasibility study suggest that it is possible to develop a small scale coaxial micro rotorcraft weighing approximately 100 grams, and that available moments are appropriate for roll, yaw and lateral control. A prototype vehicle was built and its rotors were tested in a custom hover stand used to measure Thrust and power. The radio controlled vehicle was flown untethered with its own power source and exhibited good flight stability and control dynamics. The best achievable rotor performance was measured to be 42%.

Introduction

Recent advances in electrical and mechanical system miniaturization have spurred interest in finding new solutions to an array of military and civilian missions. One such solution is the Micro Air Vehicle (MAV).[1,2] These vehicles are an order of magnitude smaller than previously developed systems and operate in a unique aerodynamic regime involving low Reynolds number flow conditions (see figure 1). Due to their unique capabilities, MAVs are applicable to such missions as covert imaging, biological and chemical agent detection, battlefield surveillance, traffic monitoring, and urban intelligence gathering. Rotary wing vehicles have significant advantages over fixed wing vehicles for these types of missions, particularly when the vehicle is required to remain stationary (hover) or maneuver in tightly constrained environments (see figure 2). For example, intelligence gathering around or within buildings requires a hovering vehicle with good maneuverability characteristics. It is important to point out that a rotorcraft maintaining hover consumes approximately twice the power of a similarly loaded, forward moving, fixed-wing vehicle. However, it is expected that recent advances in both battery and novel power supply technology (e.g. fuel cell) will allow reasonable endurance to be achieved without sacrificing hover capability. Hovering vehicle possibilities include conventional rotorcraft, ducted fans, and coaxial rotors.

This paper presents an initial design and analysis of a prototype rotary wing MAV called MICOR (MIcro-

*Send correspondence to djpterp@eng.umd.edu.

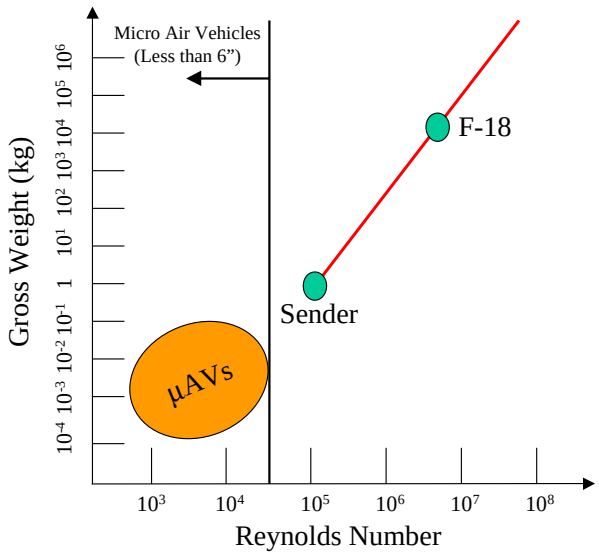

Figure 1: Relative Magnitudes of Various Aircraft.

COaxial Rotorcraft). MICOR has been designed to exploit the advantages of rotary wing configurations and is expected to be best suited to missions where hover performance is desired. The optimal mission would require that the vehicle be delivered close to the point of interest. The vehicle would then be able to investigate the target, e.g. fly through a building or hold position outside a window, while sending information back to the operator.

Design Requirements

To establish performance and design requirements, the decision was made to conform to the definitions employed by the DARPA MAV program initiated in 1996.[3] Thus, the overall dimensions of the MAV were restricted to less than 6 inches (15.24 cm) in length, width or height. A gross takeoff weight of approximately 100 grams was set as the target weight for the MAV design. A specific sensor was not selected, however the payload weight was selected to be nominally 10 grams.

In addition, it was decided that the baseline MAV design would be restricted to a rotary wing configuration. Hence, the vehicle was required to have good hover performance over an altitude of 100 meters. Extended range requirements were not set for the MAV design since efficient forward flight is not a strength of a rotorcraft configuration. It is anticipated that, in a situation where the target is far from the point of origin, an external delivery method (e.g. a mothership UAV or large scale munition) might be employed to transport the MAV. In order to facilitate delivery, the vehicle must be compactly packaged and able to withstand high g-loading. Finally, the MAV design should fulfill these requirements with a minimum of mechanical complexity. Table 1 summarizes some additional requirements for the baseline MAV considered in this study.

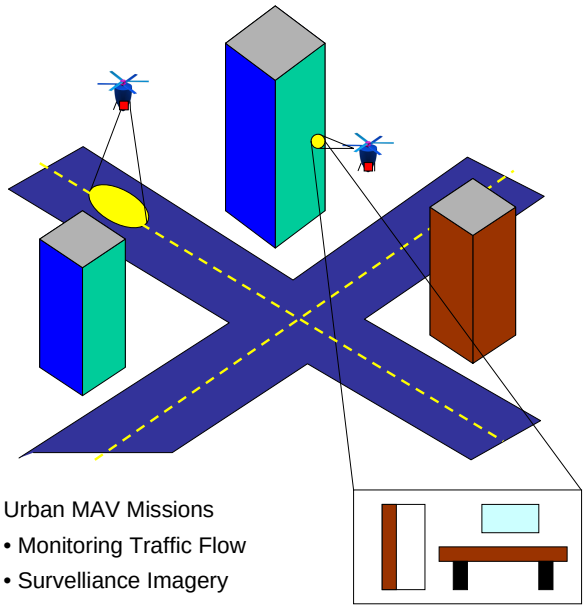

Figure 2: MAV Mission Scenario.

Desired Hover Time	20 to 30 minutes
Payload Weight	10 grams
Gross Takeoff Weight	100 grams
Altitude	100 m
Size	$\leq$ 15.24 cm
Navigation	Line of Sight tracking from ground

Table 1: Baseline MAV Design Requirements.

Concept Selection

In order to select a configuration for the vehicle different concepts were systematically compared. Selection was made following the main criteria listed below:

- Hover efficiency
- Compactness of folding
- Ease of payload packaging
- Simplicity of structure
- Controllability
- Maneuvrability

The configurations under consideration can be broken into four categories: single rotor, twin rotor, quad rotor/other rotor configurations, and hybrid helicopter configurations.

Single rotor configurations: The single rotor configurations studied are conventional main rotor/tail rotor, rotors with vanes in the slipstream for providing anti-torque,[8] and tip-jet driven rotors.[9] The first two of these configurations have been successfully tested for UAVs and MAVs .[8,10]

The conventional main rotor/tail rotor design provides good aerodynamic efficiency and has good controllability and maneuvrability. However, compactness in folding is adversely affected by the tail boom and the large size of the rotor required. Tip-jets, though at-

tractive due to their simplicity of structure and ease of payload packaging, due to the absence of a powerplant inside the fuselage, have the drawback of poor controllability. This may be attributed to the lower Lock number of the blade, due to the high blade inertia resulting from blade mounted nacelles. Finally, the vanes in the wake of the rotor working as antitorque devices, add weight and make the vehicle larger and harder to pack.

Twin rotor configurations: Four twin rotor configurations were considered: coaxials, side-by-side rotors, tandems and ducted coaxial configurations. Coaxial configuration has been widely used for UAV design, for which Sikorsky's Cypher and Cypher II[11] are good examples. The coaxial design is favored by most of the key design criteria: compactness of folding, simplicity of structure and ease of packaging. Side-by-side and tandem configurations have similar ratings. Their hover efficiency is higher than that of the coaxial configuration due to the smaller adverse wake interference between the rotors. However, the difficulty of folding and the complexity of the structure and transmission are among the key drawbacks of these configurations. Ducted coaxial design are well suited for MAVs, but have significant compactness problems. Shrouds and ducts cannot be packed efficiently making it difficult to fit the MAV into a launching vehicle.

Quad rotor and other rotor configurations: Recently, there has been an interest in the rotorcraft industry in designing rotorcraft with four or more lifting rotors. Such configurations could be controlled by varying the RPM of different rotors to change the direction of the thrust vector. Some small scale examples include the Mesicopter,[12] the Gyronsaucer and the Roswell Flyer. The latter two are commercially available RC helicopters and are reported to have very good controllability. The Mesicopter, a meso-scale flying machine which is no larger than a penny, is still in the development stage. A quad rotor design with free flying rotors can have good hover efficiency with good handling and control characteristics, so it has the potential to meet the design criteria.

Hybrid helicopter configurations: The candidates in the compound helicopter category are a rotor wing or stopped rotor, tilt-rotor, tilt-wing, joined wing, and toroid rotor configurations.[14] All these designs prove difficult to fold because of the large size of their lifting surfaces. They are all well suited for payload packaging and also very effective in high speed forward flight. However, as the mission plan does not require high speed forward flight, these designs are not suitable options for our vehicle.

From the previous comparisons it can be concluded that the conventional single rotor/tail rotor configuration, the quad rotor and the coaxial design, are the best candidates for the present design problem. The coaxial configuration has the advantages of compactness of folding and ease of deployment while the quad rotor is superior from a controllability view point. However, given the strength of the compactness requirement, the folding problems associated with the quad rotor preclude its use in this application. Hence, the final configuration chosen is that of a coaxial rotorcraft.

Vehicle Configuration

The prototype vehicle, displayed in figure 3, has a coaxial rotor configuration with an axi-symmetric fuselage. As mentioned before, the coaxial configuration is employed since it is compact, reduces net rotor size for a given gross weight and provides anti-torque capability. Because of this anti-torque capability, a tail rotor supported by a tail boom is not needed for yaw stabilization, and all power can be devoted to useful vertical lift. Additionally, to further simplify the mechanical design, the swashplate is eliminated and the rotors are completely rigid during flight.

Because the system has no swashplate or tail rotor, a non-traditional control scheme has to be employed for the roll, pitch and yaw axes. Each rotor is driven by a separate motor, which allows yaw control to be performed by varying the difference in rotational speed between the two rotors. This changes the torque transmitted to the fuselage. For control of vertical velocity, total thrust is adjusted by varying the motors' rotational speeds simultaneously.

Different lateral control methods can be considered for MICOR: aerodynamic flaps or fins to deflect the downwash of the rotors, as well as a gimballed drive-train/rotor for thrust vectoring, and ducted fan and/or reaction jets to impose rolling and pitch moments. The selection of any of those methods will influence the configuration of the vehicle. Control issues are studied in detail in a further section.

Detailed Design

The prototype Micro Coaxial Rotorcraft (MICOR) vehicle was conceived to meet the design requirements in the least complex manner. Hence, commercial off-the-shelf components were used whenever possible. However, many components were custom designed, machined and fabricated prior to assembly.

Propulsion

With the baseline design requirements previously mentioned a minimum total thrust (produced by the two rotors) of 100 grams is needed to hover. Assuming a conservative Figure of Merit of 50% for a small scaled rotor, the required baseline shaft power for hover for each rotor is 3 watts. If an electric motor-transmission system is chosen with a 65% efficiency, the baseline electrical power required is approximately 4.5 watts. Because of the separation between the two rotors, in theory, for fully developed upper rotor wake, half the area of the lower rotor operates in an effective climb velocity.As a result, the induced power is increased by a factor of approximately 1.28 the induced power with respect to the case of two independent rotors producing the same thrust. The overall power required for hover is then 11.5 W. To ascend and maneuver, at least an extra 25% of this power is needed. Thus, 15 watts of available power was set as a design requirement.

To produce this power,[6] a variety of options are available including electric motors, internal-combustion engines, turbines, thermopiles, chemomechanical engines, remote powering methods, fuel cells and compressed gas. Of these power/propulsion options, fuel cell technology and new flexible lithium batteries appeared to be the most promising for future MAVs. However, few, if any of these systems have been built for small scale vehicles. The most readily available clean and efficient propulsion option is battery driven electric propulsion.

The batteries selected for the MICOR are three 3-volt Lithium $LiMnO_2$ cells, with a capacity of 430 mAh. Assuming an average power consumption of 13 watts, and a constant operating voltage of 9-volts, the current drain of the system is 1.45 amperes. If the batteries are capable of providing this constant current flow, then the MICOR would fly for 17 minutes. However, one drawback of this commercial battery is its poor discharge rate. Thus, it is unlikely that this battery will be able to maintain the required current flow for a long time. Nevertheless, it was chosen in this initial design study. The electric motor chosen for the MICOR configuration was a commercial off-the-shelf 9-volt coreless DC motor. This motor was chosen for its high power output as compared to other electric motors of similar size and weight (see table 2).

Rotor Blades and Hub

Curved plate airfoils have relatively good aerodynamic performance at low Reynolds numbers,[4,5] plus they are easy to manufacture. Hence, a thin curved plate airfoil with 8% constant radius camber was chosen. Each blade has a chord of 1 cm and a length of 7 cm (constrained by the overall vehicle size requirement). The blades consist of three layers of graphite/epoxy weave prepreg with a layup of (+45,0,+45). A simple mold composed of a top concave surface, a bottom convex surface, and an edge dam was machined from aluminum (see figure 4).

The composite was placed in the mold, clamped and cured. The resulting blades are very consistent and require only minimal post cure processing. Finally, a small aluminum pin was bonded to the root of the blade. The root pin has a flat surface along a portion

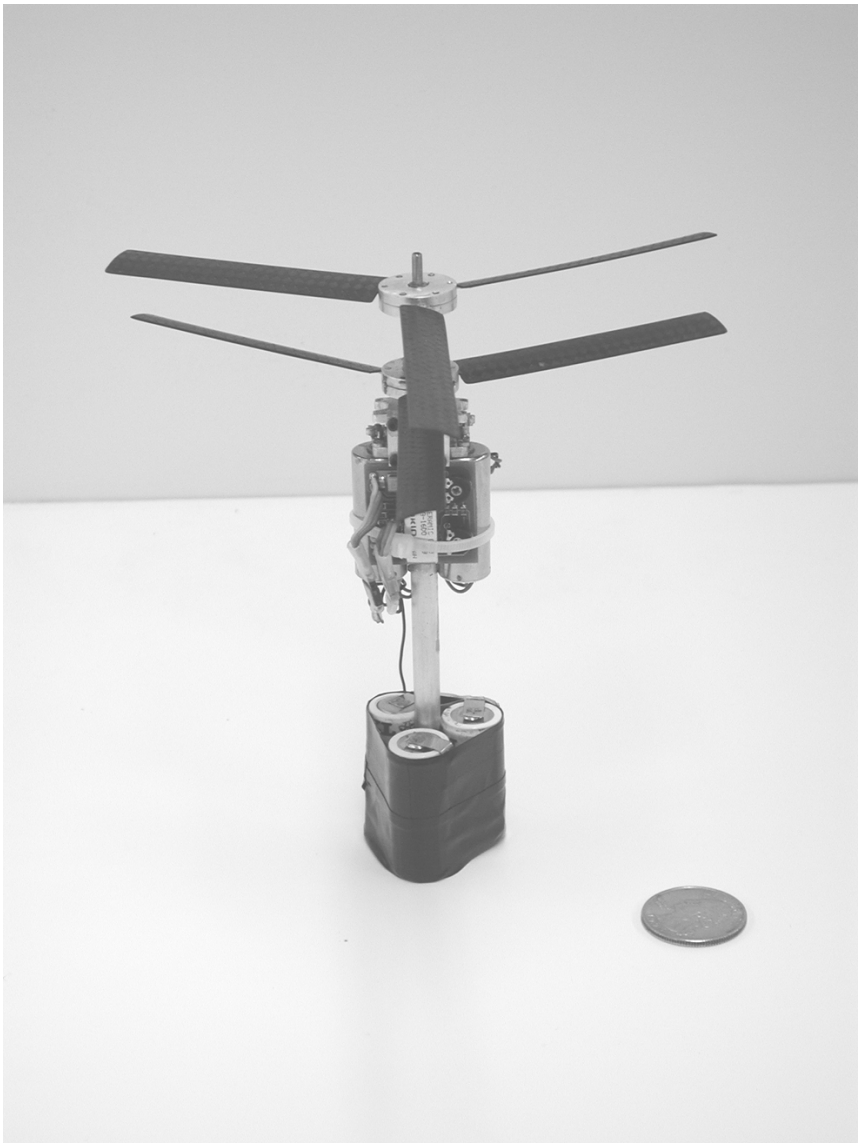

Figure 3: MICOR Prototype.

Parameter	**WES-Technik*** **DC 6-8.5**	**WES-Technik DC 5-2.4**	**MicroMo DC 1717**
Rated Voltage (V)	6	5	3
No Load Speed (rpm)	25200	21000	12600
Stall Torque (g-cm)	131	44.8	39.7
Maximum Output Power (W)	8.52	2.42	1.41
Maximum Efficiency (%)	77.3	75.3	66
Weight (g)	17	10	17

*Motor Chosen for MICOR

Table 2: Motor Performance Comparison.

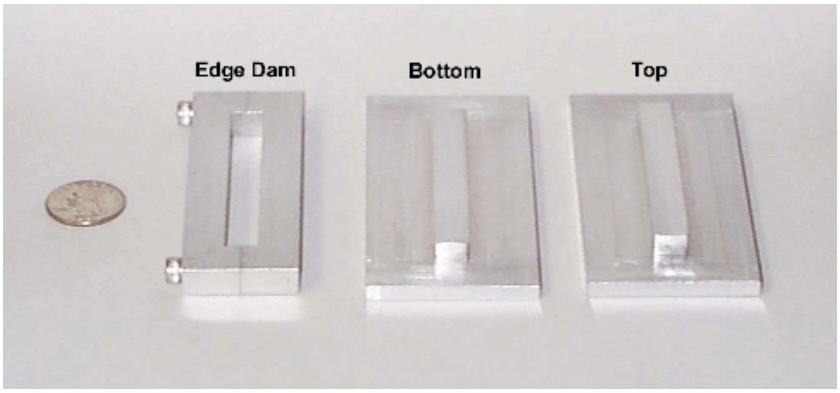

Figure 4: Blade Mold Parts.

of its length to aid in bonding, and the opposite end is flared to transfer axial loads from the blades to the hub.

The rotor hub consists of two parts, top and bottom, that clamped onto the root pin, constrain its rotation and thus fix the angle of attack of the blades. A space was left in the hub for the flared end of the root pin. This design allows the blade angle of attack to be changed between tests. Future rotor designs might incorporate embedded actuators and sensors to permit individual rotor geometries to be varied adaptively.

System Integration

The vehicle configuration requires that each rotor be driven by a separate motor. However, the rotors are coaxial while the motors are not. The motors are mounted parallel to the axis of rotation of the rotor shafts. Each motor/rotor system consists of a pinion mounted to the motor shaft that in turn drives a gear attached to the rotor shaft. In order to let the shaft axis of rotation for each rotor be coaxial, the gears, and thus the pinions, must be offset vertically. Since the motors are not coaxial, the pinions must also be offset horizontally, with each pinion being coaxial with its corresponding motor. The transmission housing was designed to support the gears, rotor shafts and motors, and transmit the rotor loads from the rotor system to the rest of the structure. The primary structural member is a thin walled shaft mounted to the bottom of the transmission housing. This shaft gives support for the motors, batteries, required electronics and payload. The resulting configuration is shown in figure 5. The final transmission design consists of an 8 tooth pinion and a 30 tooth gear, resulting in a reduction ratio of 3.75:1. In addition to having the desired reduction ratio, this configuration provides enough space between the motors for the structural shaft.

Flight Control

A fully functional flight control is an absolute necessity for MICOR, given the mission requirements specified by DARPA. A typical rotorcraft control system (swashplate, pitch links, etc.) is quite complex; this is especially true for a coaxial rotor configuration. However, this complexity is prohibitive as it would significantly decrease the reliability and survivability of the vehicle. To simplify the mechanical design, the swashplate is eliminated and the rotors are completely rigid during flight. Hence, a non-traditional flight control system must be developed.

Yaw and Thrust Control

Yaw control and thrust (altitude) control can be accomplished by varying the RPM of the rotors. Yaw

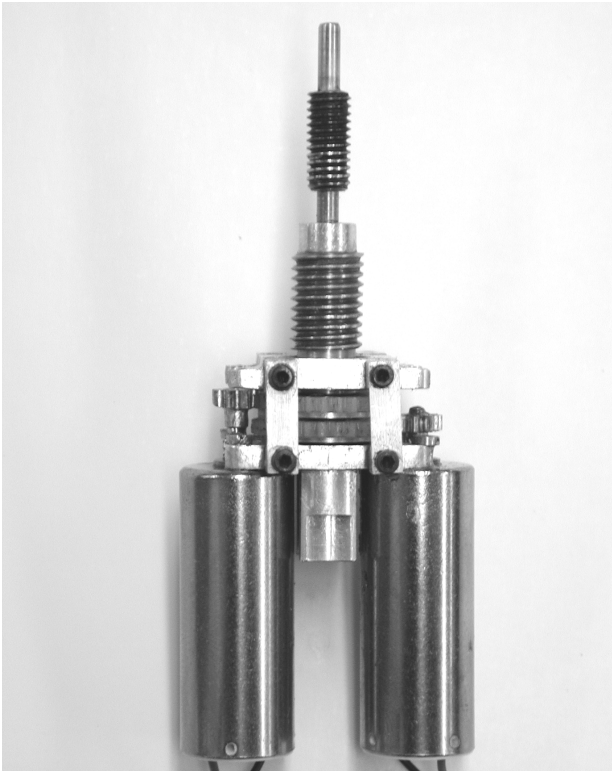

Figure 5: MICOR Transmission Configuration.

control can be performed by varying the difference in rotational speed between the two rotors, creating a torque applied to the fuselage. Thrust is adjusted by varying the rotors' RPMs equally.

Lateral Control

A number of lateral control methods were considered for MICOR, including aerodynamic surfaces (flaps), a gimballed drivetrain/rotor for thrust vectoring, and ducted fan and/or reaction jets to impose rolling and pitch moments. These three proposed systems were considered from the standpoints of mechanical complexity, control algorithm complexity, and power required. The control systems are shown in figures 6, 7, and 8, respectively.

Of the three systems, the aerodynamic flap system would be the easiest to implement and seemed to require only a small amount of power to operate. A more traditional control scheme would be to use fins that are mounted perpendicular against the fuselage, extended into the rotor downwash. However, flap control was chosen over fin control for two reasons. First, the flap system is more compact since, except during maneuvers, the flaps remain flush to the fuselage. Second, when not maneuvering, the flaps remain out of the rotor downwash and thus drag is reduced and hover efficiency is increased. Extension of the flaps creates a torque which is used to control the attitude of the vehicle in pitch and roll. Development of stability and control algorithms using this control method was determined to be a tractable problem.

The gimballed rotor/motor system, though slightly more complex than the aerodynamic flap system, ultimately yields the cleanest final vehicle configuration, and potentially requires the least amount of power to operate. Once again, the development of stability and control algorithms using this control method was determined to be a tractable problem.

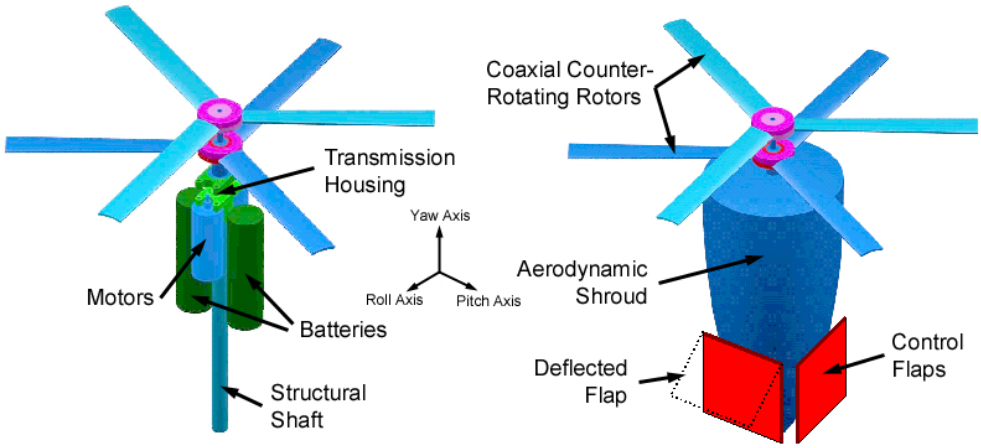

Figure 6: Aerodynamic flaps

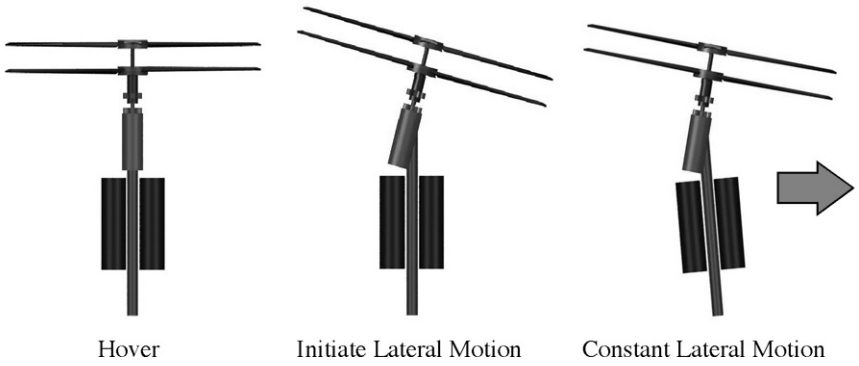

Figure 7: Gimballed drivetrain/rotor

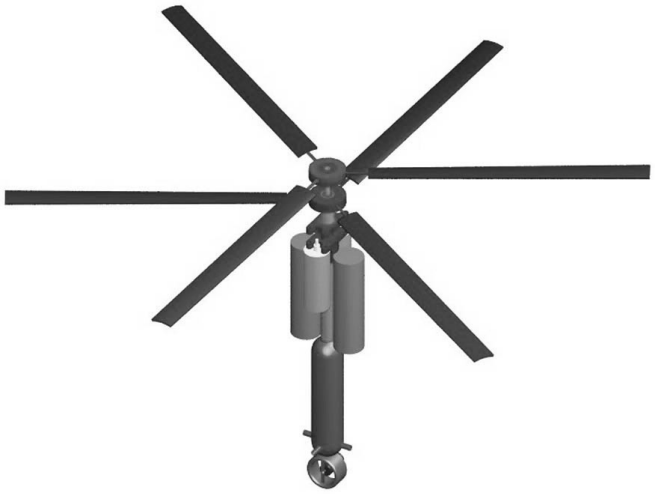

Figure 8: Ducted propeller with reaction jets

The preliminary study indicated that the ducted propeller/reaction jet system would require significantly more power than the previous two systems, so it is not considered further in this paper.

Available control moments

Two of the lateral control systems mentioned previously - flaps mounted flush to the fuselage and a gimballed drivetrain rotor (hinged mass) - have been studied for MICOR. First, the pitch/roll moments each configuration can generate are estimated for a general vehicle, then values for disturbance moments generated by gusts are estimated. In the hinged mass configuration, the plane of the rotor system is tilted with the use of servos, thus reorienting the thrust vector and causing body moments. In the aerodynamic flap configuration, moments are generated by deflecting flaps into the rotor downwash.

The following analysis predicts the magnitude of the moments that each system can generate, and then discusses whether or not we expect these moments to translate to sufficient bandwidth for a coaxial rotorcraft in a noisy environment. All the analysis is performed for the simplified case of the vehicle in hover.

The moment generated by a deflection of the thrust vector by Θ_T degrees and moment arm d_T is

$$M_T = d_T T \sin\Theta_T \tag{1}$$

Typical values for MICOR are easily found. Thrust equals the weight of the system, approximately one Newton. To maximize available moments in this configuration, the heaviest components would be placed near the bottom of the vehicle to maximize d_T. Assume a d_T of 10 cm is achievable. Lastly, a typical value must be chosen for Θ_T. Considering that for practical purposes we don't want the vertical component of thrust to change by more than a few percent, a generous upper bound for Θ_T is 15 degrees. Therefore, substituting in these values, the maximum expected moment is

$$M_T = .026 \text{ Newton-Meters} \tag{2}$$

For the aerodynamic flap configuration, the moment generated by a fin force F_f is simply $d_f F_f$ where d_f is the effective arm . If we assume that the flaps have a constant lift curve slope of $C_{l\alpha}$ then the moment for a flap deflection of α becomes $\frac{1}{2} d_f C_{l\alpha} \alpha \rho V^2 A_f$, where V is the local wind velocity and A_f is the surface area of the flap. If we further assume that the flaps operate in the fully contracted rotor wash, then from simple momentum theory V becomes $\sqrt{\frac{2T}{\rho A}}$, where ρ is the air density and A_r is the surface area of the rotor disk. Therefore, the total moment due to the flaps can be written

$$M_f = \frac{T A_f d_f C_{l\alpha} \alpha}{A} \tag{3}$$

For this configuration, we would place the center of gravity of the vehicle as close to the rotors as possible, and place the flaps far from the rotors. With this strategy a d_f of 10 cm should be achievable. Given a typical rotor diameter of 15 cm, air density at sea level of $1.225 \frac{\text{kg}}{m^2}$, flap surface area of 50 cm^2, lift curve slope of 2π per radian and a maximum flap deflection of 30 degrees, the expected maximum moment due to flaps at hover is

$$M_f = .035 \text{ Newton-Meters} \tag{4}$$

The typical fin surface area of 50 cm^2 is generated by assuming two fins of surface area 25 cm^2, on either side of the fuselage and deflecting in the same direction. If the flaps are mounted flat against the fuselage such that only one could be deflected, the available moments are cut in half.

Considering the simplified nature of moment approximations, the one third greater estimated moment of the flap configuration is somewhat negligible. The interesting result is that each configuration produces moments of approximately the same magnitude, at around a few hundredths of a Newton-meter. A more detailed analysis would consider numerous additional factors, including better approximations of the rotor wash velocity and available flap forces. In practice, it is easier to move the center of gravity closer to the rotor than further away since the transmission and motors must necessarily be located near the rotor. This tends to favor the aerodynamic flap configuration.

Now that the approximate magnitudes of the available moments are known, the next logical step is to determine if these moments are large enough to attenuate the disturbance moments acting on MICOR. The primary disturbance source is wind gust. Because the vehicle is so small and dense, disturbances are relatively small. An approximation of the order of magnitude of gust disturbances can be generated by modeling MICOR as a cylinder. The moment acting on a cylinder in a gust can be written as:

$$M_g = \frac{1}{2} C_d \rho V_g^2 A_g d_g \tag{5}$$

Where C_d is the drag coefficient, ρ is the air density, V_g is the gust velocity, A_g is the reference area and d_g is the moment arm. For MICOR, $C_d = 1$, $\rho = 1.225 \frac{\text{kg}}{m^2}$, $A_g = 0.003\ m^2$ and $d_g = .05\ m$. Using these values and a large gust velocity of $5 \frac{m}{s}$ yields a gust moment of 0.0023 Newton-Meters, which is an order of magnitude lower than the achievable command moments.

Hover Performance

While the hover performance of more conventional full-scale rotorcraft configurations is well documented in the literature, the hover performance of micro air vehicles in hover at low Reynolds numbers[7] is relatively unknown. Thus, the baseline MICOR vehicle was flown in a laboratory environment and its rotors were tested in a custom designed hover stand to evaluate its performance

Mathematical Models

In estimating the efficiency of low Reynolds number rotors in hovering flight, it is important to consider losses that affect hover performance including profile drag, nonuniform inflow, slip stream rotation, and tip losses. Following simple momentum theory, the thrust generated from a rotor in hover can be written as

$$T = \dot{m} 2 \nu_i = \left(\rho \pi R^2 \nu_i\right) 2 \nu_i = 2 \rho A \nu_i^2 \tag{6}$$

where ν_i is the induced velocity through the rotor disk, $\dot{m}$ is the mass flow rate trough the rotor, ρ is the air density and R is the rotor radius. In estimating the effectiveness of a lifting rotor in the hovering condition, it is not possible to apply the propeller criterion of efficiency given by

$$\eta = \frac{useful power}{total power} = \frac{P_{out}}{P_{in}} = \frac{TV}{P} \tag{7}$$

Because a standard is needed to judge the effectiveness of a rotor in producing thrust in a zero axial flow field, a different criterion of efficiency has to be introduced. In the hovering flight condition, power is expended in producing thrust T, while the axial flow velocity seen by the rotor V is zero. This would imply a propeller efficiency of 0. Thus, the lifting rotor needs some other measure of efficiency to judge lifting capability. This is accomplished by comparing the actual power required to hover with the ideal power required to hover. This leads to the rotor Figure of Merit, FM, given by

$$FM = \frac{ideal\ hover\ power}{actual\ hover\ power} = \frac{T \nu_i}{P} \tag{8}$$

The larger the value of FM, the smaller the power required to produce a given thrust, or the larger the thrust per unit power. For an ideal rotor FM should equal 1. However, this is based on the assumption of uniform inflow conditions, zero-profile drag, and no tip losses. The induced (ideal) power required to hover is given by $P = T\nu_i$. This means that the ideal power loading is inversely proportional to the induced velocity at the disk. By rearranging equation 8 it is not difficult to derive the following equation relating power loading to rotor disk loading as a function of FM.

$$P.L.^{-1} = \frac{\sqrt{D.L.}}{FM\sqrt{2\rho}} \tag{9}$$

where

$$P.L. = \frac{T}{P} \tag{10}$$

$$D.L. = \frac{T}{A} \tag{11}$$

This equation is useful for estimating rotorcraft hovering performance. In nondimensional form equation 8 can be represented as

$$FM = \frac{C_T^{3/2}}{C_P \sqrt{2}} \tag{12}$$

where C_T and C_P are the thrust and power coefficients, respectively. The FM can be used as a measure of the efficiency of a rotor generating thrust for a given power. However it should only be used as a comparative measure between two rotors at the same thrust coefficient. The thrust, torque and power are given by

$$T = C_T \pi R^2 \rho (\Omega R)^2 \tag{13}$$

$$Q = C_Q \pi R^2 \rho (\Omega R)^2 R \tag{14}$$

$$P = C_P \pi R^2 \rho (\Omega R)^3 \tag{15}$$

While simple momentum theory can be used to estimate the efficiency of rotors , a more accurate aerodynamic theory is needed to incorporate blade geometry, sectional orientation and twist condition. Blade element theory evolved to incorporate the effects of drag and twist on rotor performance. This theory permits the derivation of the following equations for the thrust and torque coefficients.

$$C_T = \frac{1}{2}\sigma C_{l\alpha}\left(\frac{\theta_{75}}{3} - \frac{\lambda}{2}\right) \tag{16}$$

$$C_P = \frac{C_T^{3/2}}{\sqrt{2}} + \frac{Cd_0\sigma}{8} \tag{17}$$

Where θ_{75} is the blade pitch angle taken at 3/4 radius, λ the rotor inflow ratio ($\frac{v_i}{\Omega R}$ for hover), Cd_0 is the average drag coefficient and σ is the rotor solidity, given by:

$$\sigma = \frac{N_b c}{\pi R} \tag{18}$$

In order to include the non ideal aerodynamic effects such as non uniform inflow, tip losses and wake swirl, the empirical coefficient κ known as the induced power factor should be included in the induced power expression. Substituting equation 17 into equation 12, leads to the following expression of FM.

$$FM = \frac{\frac{C_T^{3/2}}{\sqrt{2}}}{\kappa\frac{C_T^{3/2}}{\sqrt{2}} + \frac{\sigma Cd_0}{8}} \tag{19}$$

Experimental Setup

In order to determine the performance of MICOR's rotors for a range of thrust coefficients, a hover test stand was designed and built. The test stand, shown in Figure 9, is an instrumented platform where the MAV's motor-transmission system is mounted with one or two rotors, via a stem. The rotors are inverted so that the air flow goes from bottom to top. This avoids any In Ground Effect (IGE) and simplifies the thrust measurement (directed downwards).

Thrust and moment are measured using two load cells. The transmission's support can rotate freely and moment is transmitted to a load cell by a 1 inch arm. Thrust is measured by the second load cell placed directly under the platform's shaft. Each rotor's rotational speed is determined using a Hall effect sensor that remains stationary while a pair of rotating magnets attached to the hub produce an output signal every time they pass over it. The number of peaks in the output signal over a period of time is then proportional to the rotational speed. Additionally, the voltage and current supplied to the motors are also measured to obtain the electrical power consumption.

All the data was acquired and processed by a data acquisition system linked to a computer running LabView, so that an acceptable level of accuracy could be attained in all the measurements.

Experimental Results

Two main sets of experiments were performed: single rotor with twisted and untwisted blades, and coaxial configuration with untwisted blades. For the single rotor tests the collective pitch was increased from 6 to 18 degrees in steps of 3 degrees. In the coaxial configuration tests, three angles of attack settings were tested: 15 degrees lower and upper rotors, 18 degrees lower and upper rotors, and 15 and 18 degrees upper and lower rotors respectively.

Single rotor tests: For every angle of attack rotational speeds were varied between 3000 and 4500 RPM. In figures 10 and 11 all the FM values are shown for twisted and untwisted blades respectively. Notice that the FM increases with increasing thrust coefficient and pitch angle of attack. This increase in FM is attributed

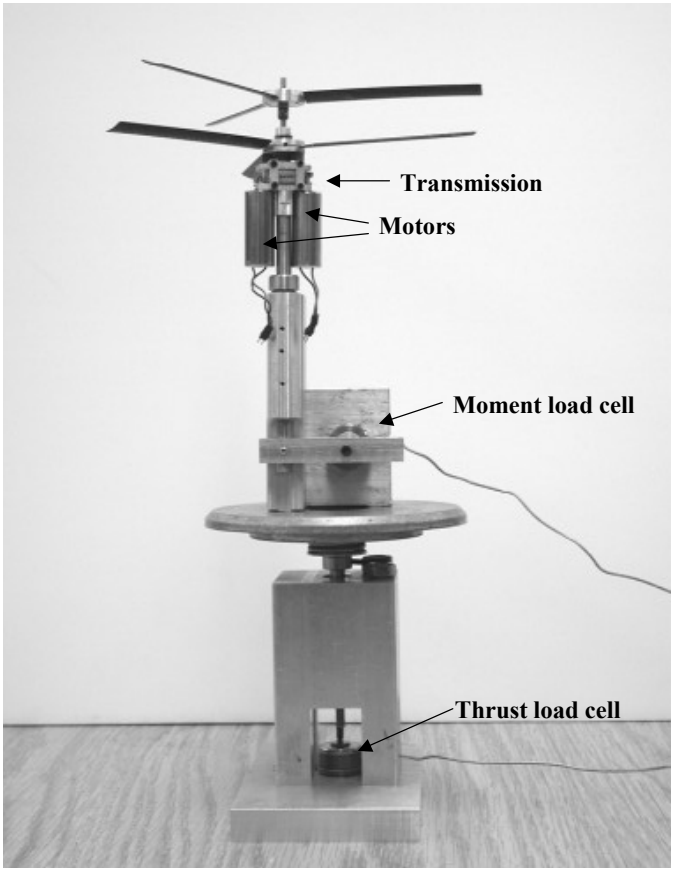

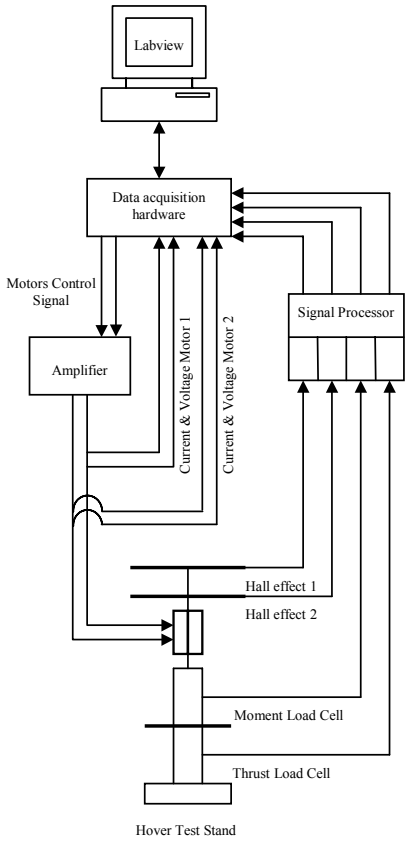

Figure 9: Hover Stand and Circuit Sketch

	15-15 pitch angle of attack			**15-18 pitch angle of attack**			**18-18 pitch angle of attack**		
	RPM	P_{elec} (W)	Thrust (g)	RPM	P_{elec} (W)	Thrust (g)	RPM	P_{elec} (W)	Thrust (g)
Upper Rotor	4517	8.1		3930	7.8		4000	8.17	
Lower Rotor	4548	7.8		4249	8.1		4041	8.23	
Total		15.9	110.26		15.9	112.57		16.5	110.15

Table 3: Coaxial Tests Results.

to the rotor overcoming the profile drag term dominant at low thrust values.

In general the highest FM for every angle of attack is obtained at the highest rotational speed. In figure 12 only these maximum values are plotted, and the results for twisted and untwisted blades are compared. The use of twist in the rotor blades gives a more uniform inflow, and reduces the induced power. The 10 degrees linearly twisted blades should theoretically increase the FM by a value close to 5%. However uniform twist does not yield as great a performance gain as predicted by the theoretical calculations. Experimental results show that there is no significant difference between the twisted and untwisted rotors. The error bars are three standard deviations long, so it is possible that the beneficial effects of the twist cannot be observed since they have a similar magnitude to that of the error.

The highest Figure of Merit values ($FM = 41.5\%$) were obtained at around 4500 RPM and 15 degrees pitch angle of attack, which corresponds to a C_T of 0.165. Thrust values of 60 grams were measured with around $8W$ of electric power consumption. This can be chosen as the hover operating point of the vehicle since it is close to the design requirements.

The rotor's tip Reynolds number is around 30,000. For such a low Reynolds number there is a degree of uncertainty in the value of the drag coefficient, Cd_0, and in the induced power factor, κ . Experimental and numerical simulation studies suggest that Cd_0 for conventional NACA series airfoils and curved plates at low Reynolds numbers may range from 0.02 to 0.1.[4,5] The actual value depends on the viscous drag effects, blade geometry and surface roughness of the manufactured airfoils. For curved plates a conservative value of Cd_0 is 0.1. Assuming this to be the drag coefficient of the rotor blades the induced power factor should be equal to 1.42. In a full scale helicopter κ is around 1.15. A value of 1.42 shows the importance of aerodynamic losses in the system, and consequently producing the extremely low Figures of Merit obtained by the prototype. To avoid the estimation of the drag coefficient, wind tunnel tests are going to be performed on MICOR's blades at the corresponding Reynolds numbers. The lift and drag coefficients obtained will allow an accurate calculation of the induced power factor.

Coaxial configuration tests: For the tests performed in the coaxial configuration, the current supplied to the upper rotor was chosen, and then the voltage given to the upper rotor was set such that there was no net torque applied to the fuselage. Then the total thrust, and each rotor's rotational speed were measured. The obtained results are shown in table 3.

For the different collective pitch settings tested, relatively small differences were found. The collective pitch combination that produced the most thrust was the 15 degrees upper rotor, 18 degrees lower rotor. Due to the wake of the upper rotor, the lower rotor will have a reduced effective angle of attack, so it is convenient to set its collective pitch higher than the optimal. The total power consumption was similar to that of the $15-15$ degrees case, however 2 extra grams of thrust were produced. The $18-18$ arrangement gave similar thrust values than the $15-15$ arrangement, but with higher power requirements. Finally, the tested rotors in the coaxial configuration at $15-15$ degrees pitch angle of attack yielded a measured thrust capability of 110 grams. This is around 5% less than twice the value obtained in the single rotor tests at the same rotational speed. Simple momentum theory predicts a thrust production of the second rotor of 76% the nominal value. This is equivalent to an overall thrust reduction of 12% for a fully developed upper rotor wake. A flow visualization experiment as well as a reduction in the error in the experimental measurements would be appropriate to obtain an explanation and better understanding of this phenomenon.

Test flights: The prototype has an overall takeoff weight (without sensor) of 100 grams, 10 more grams than the baseline requirement. The batteries account for 40% of the total weight, making them the heaviest component of the vehicle. Since lateral control has not been implemented, the prototype was tested in vertical flight using a nylon string for guide. The efficiency of the motors-transmission system was measured to be 60%, 5% lower than the estimated initial value. As expected the large current draw of the system considerably reduced the performance of the batteries, lead-

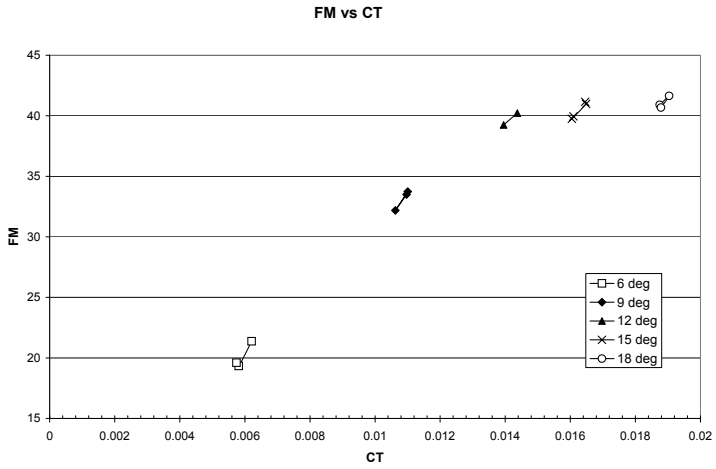

Figure 10: Untwisted Blades: Experimental Figure of Merit vs. C_T

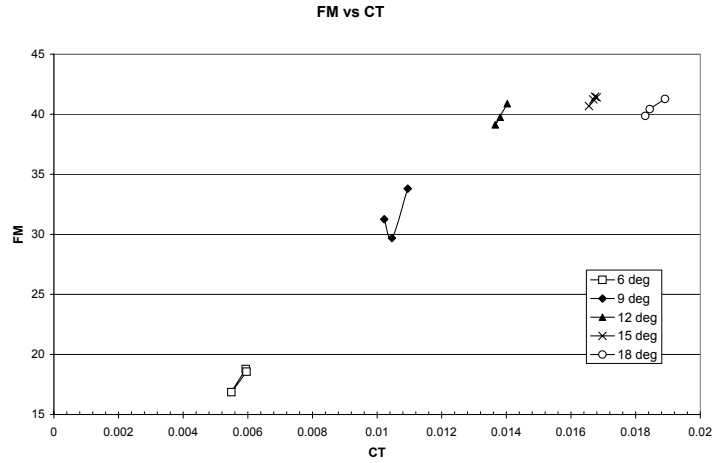

Figure 11: Twisted Blades: Experimental Figure of Merit vs. C_T

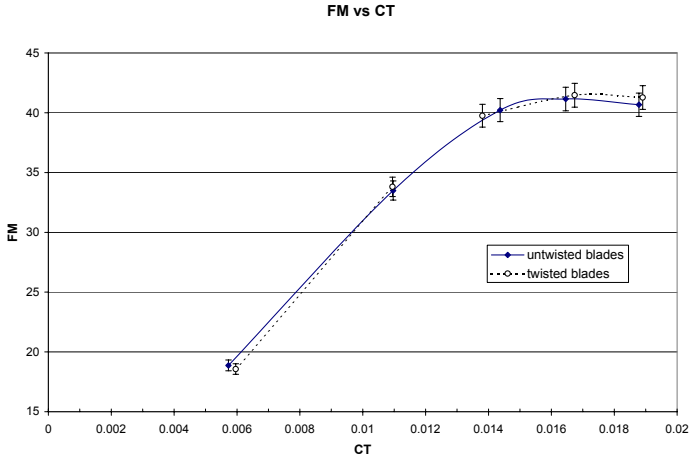

Figure 12: Twisted and Untwisted Blades, Experimental Figure of Merit vs. C_T

ing to hover times of only 3 minutes instead of the 17 minutes initially predicted.

During the test flights the MICOR prototype demonstrated good handling qualities as well as satisfactory open loop altitude and yaw controls.

Summary and Conclusions

In summary, an initial design of a coaxial micro rotorcraft configuration has been developed and flight tested. The prototype design, called MICOR, weighs approximately 100 grams without a fuselage or lateral control fins. No length dimension of the vehicle exceeds 6 inches. Preliminary flight testing of the MICOR vehicle under autonomous power demonstrated vertical ascent capability along with open loop differential yaw control. Flying times of three minutes were reached using three 430 mAh, 3-volt $LiMnO_2$ Batteries. Aerodynamic performance of the rotors was poor yielding a Figure of Merit of approximately 42% for a set of twisted blades. Much work is needed to improve the aerodynamic performance of the coaxial rotors and reduce the adverse effects of viscous drag at low Reynolds number. Surface roughness and poor choice of rotor blade planform shape contributed to poor aerodynamic performance. Future work will consist of an improved rotor blade design, an improved hover test stand, flow visualization and payload integration.

Acknowledgements

The authors would like to thank Bernard LaFrance for his mechanical insights.

References

[1] Davis, W.R.,"Micro UAV," Presentation to 23rd Annual AUVSI Symposium, 15-19 July, 1996.

[2] Davis, Jr., W.R., Kosicki, B.B., Boroson, D.M., and Kostishack, D.F., "Micro Air Vehicles for Optical Surveillance", The Lincoln Laboratory Journal, Vol. 9, No. 2, 1998.

[3] Hundley, R.O. and Gritton, E.C., "Future Technology-Driven Revolutions in Military Operations-Results of a Workshop," RAND National Defense Research Institute, December, 1992.

[4] Bruining, A., "Aerodynamic Characteristics of a Curved Plate Airfoil Section at Reynolds Numbers 60,000 and 100,000 and Angles of Attack from Minus 10 to +90 Degrees," Technische Hogeschool, Delft (Netherlands). Dept. of Aerospace Engineering, May,1979.

[5] Pelletier, A., Mueller, T.J., "Low Reynolds Number Aerodynamics of Low-Aspect-Ratio, Thin/Flat/Cambered-Plate wings", *Journal of Aircraft*, vol 37, No 5, September-October 2000.

[6] Power Computing Solutions, "Electric Power System for High Altitude UAV Technology", NASA/CR-97-206337, 1997.

[7] Langford, J.S., "The Daedalus Project: Summary of Lessons Learned", AIAA/AHS/ASEE Aircraft Design, Systems and Operating Conference, 1989.

[8] Smith, J.O., Black, K.M., Kamangar, F.A., and Fitzer, J. "The University of Texas at Arlington autonomous aerial vehicle - an overview," *Journal of Applied Intelligence*, vol. 2, 1992.

[9] Stepniewski, W.Z. and Tarczynski. T, "Open Airscrew VTOL Concepts", NASA Contractor Report 177603.

[10] Woodley, B., Jones, H., Frew. E., LeMaster, E., Rock, S. "A Contestant in the 1997 International Aerial Robotics Competition." *A*UVSI '97 Proceedings, July 1997. Aerospace Robotics Laboratory, Stanford University.

[11] Zorpette, G. "Spying saucer. Cypher" Scientific American v. 276 (June '97) p. 40

[12] Kroo, I., Kruntz P. ”Development of the Mesicopter: A miniature Autonomous Rotorcraft”, Presented at the AHS Vertical Lift Aircraft Design Conference, San Francisco CA, 2000.

[13] Rutherford, J.W., Bass, S.M., Larsen, S.D., ”Canard rotor/wing-A revolutionary high-speed rotorcraft concept”,AIAA, AHS, and ASEE, Aerospace Design Conference, Irvine, CA, Feb. 16-19, 1993. 11 p.

[14] Stancil, Charles M. “Electric Toroid Rotor Technology Development”, Phase I study funded by NASA Institute for advanced Concepts, Nov 1, 1998 to Apr 30, 1999.